# Relation between the built-in voltage in organic light-emitting diodes and the zero-field voltage as measured by electroabsorption

R. J. de Vries,[1,2,3,*] S. L. M. van Mensfoort,[1,2] R. A. J. Janssen,[1] and R. Coehoorn[1,2]
[1]*Department of Applied Physics, Molecular Materials and Nanosystems, Eindhoven University of Technology, P.O. Box 513, 5600 MB Eindhoven, The Netherlands*
[2]*Philips Research Laboratories, High Tech Campus 4, 5656 AE Eindhoven, The Netherlands*
[3]*Dutch Polymer Institute (DPI), P.O. Box 902, 5600 AX Eindhoven, The Netherlands*
(Received 19 November 2009; published 9 March 2010)

For developing understanding of the current density onset voltage and injection barriers in organic light-emitting diodes (OLEDs), a precise determination of the built-in voltage, $V_{bi}$, is of crucial importance. Commonly, $V_{bi}$ is assumed to be equal to the voltage $V_{0,EA}$ at which in an electroabsorption (EA) experiment the reflection of light at the OLED is found to become insensitive to a small voltage modulation. However, this assumption is shown to lead to significant errors for devices with well-injecting contacts. From an analysis of EA experiments for hole-only devices containing a polyfluorene-based copolymer, it is shown that $V_{0,EA}$ may be interpreted as an effective current density onset voltage, agreeing with the commonly accepted picture, but that for these devices $V_{bi}$ is ~0.5 V larger than $V_{0,EA}$. This is found to be consistent with predictions of $V_{0,EA}$ from model calculations of the electric field and light-absorption profiles in the semiconducting layer.

DOI: 10.1103/PhysRevB.81.125203 PACS number(s): 72.80.Le, 73.61.Ph

## I. INTRODUCTION

Since the demonstration of bilayer organic light-emitting diodes (OLEDs) by Tang and VanSlyke,[1] the power efficiency of OLEDs has increased impressively.[2–4] Advances in the understanding of the relevant processes, such as charge-carrier injection, transport and recombination, are expected to enable further progress. Many of these processes are strongly affected by the electric field, $F$. In the absence of a space charge, the electric field would be uniform and given by $(V-V_{bi})/L$, with $V$ the applied voltage, $V_{bi}$ the built-in voltage and $L$ the semiconductor layer thickness. The built-in voltage may be expressed as $V_{bi}=(W_a-W_c)/e$, with $W_a$ and $W_c$ effective work functions of the anode and cathode, respectively, and with $e$ the elementary charge. $V_{bi}$ is an important parameter in device models, as it is related to the hole and electron injection barriers, $\Phi_h$ and $\Phi_e$, at the anode and cathode interfaces, respectively, via the relationship $\Phi_h+\Phi_e=E_g-V_{bi}/e$, with $E_g$ the semiconducting gap energy.

The built-in voltage may be determined using, for example, capacitance-voltage measurements,[5] photovoltaic measurements,[6] steady-state current-voltage measurements,[8] and electroabsorption (EA) measurements.[9–20] The latter method, which probes the electric field in OLEDs, is the subject of this paper. EA experiments involve measurements of the modulation, $\Delta R$, of the reflection coefficient for monochromatic light, $R$, resulting from the application of a small ac voltage superimposed on a dc bias voltage. This noninvasive technique uses the fact that the optical absorption coefficient $\alpha$ of an organic layer changes with the square of the electric field. The change in $\alpha$ is caused by a Stark-like shift in the allowed optical transitions.[21] In most analyses, it is assumed that the electric field is uniform across the organic semiconducting layer(s), at least at small voltages below $V_{bi}$. The field dependence of the absorption leads then to a field-dependent relative change in the reflection coefficient given by[9]

$$\frac{\Delta R}{R}(h\nu) \propto \mathrm{Im}\,\chi^{(3)}(h\nu)F^2. \tag{1}$$

Here, Im $\chi^{(3)}$ is the imaginary part of the third order susceptibility at the photon energy $h\nu$ employed. The photon energy dependence of the effect has been used to resolve the electric field in distinct semiconducting layers within multilayer OLEDs.[22–25] Furthermore, the photon energy and modulation frequency dependence has been used to distinguish the Stark-like effect mentioned above from a contribution due to charge-induced absorption.[15–18,24–26] The voltage $V_{0,EA}$ at which the relative change in reflection in a single-layer device vanishes is commonly viewed as a direct measure of $V_{bi}$.

In this paper, we demonstrate that for OLEDs with well-injecting contacts the assumption that at $V_{0,EA}$ the field across the semiconducting layer is essentially uniform is not correct, and that this can result in a significant difference between $V_{0,EA}$ and $V_{bi}$. The effect is caused by the presence of a substantial space-charge density close to the injecting electrodes, even at voltages well below $V_{bi}$. This affects the electric field throughout the entire device. We also argue that, in view of the nonuniformity of the electric field, it will in general be important to include the variation in the optical absorption across the semiconducting layer in the analysis. The absorption in the active layer is far from homogeneous, as is shown from thin-film optical microcavity calculations. The analysis is carried out for sandwich-type hole-only devices containing a blue-emitting polyfluorene-based copolymer with varying layer thicknesses. For the devices studied, the charge-carrier density and electric field dependence of the mobility is well-known from an analysis of steady-state current density versus voltage $[J(V)]$ measurements.[8] This makes it possible to accurately determine $V_{bi}$ from such measurements, using a drift-diffusion device model.

Section II contains a description of the material and device structures, and of the experimental methods. In Sec. III,

 

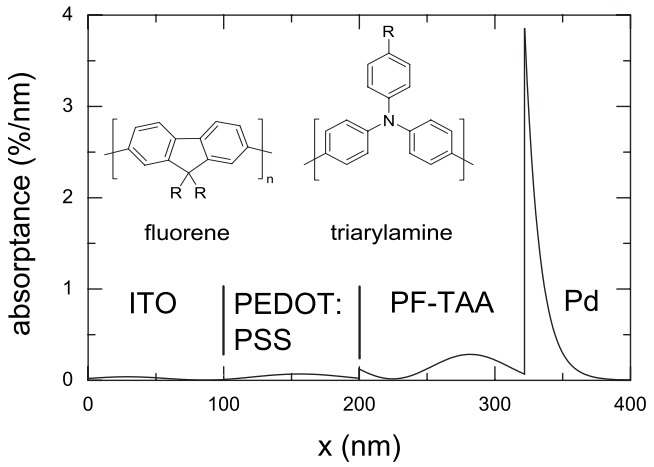


FIG. 1. Layer structure of a 122 nm device as studied in this paper, calculated absorptance as a function of the distance $x$ from the glass/ITO interface (see Sec. III), and structures of the fluorene and triarylamine monomer units forming the PF-TAA copolymer.

the experimental results are presented and analyzed. A model is developed which describes the layer thickness dependence of $V_{0,EA}$, the difference with $V_{bi}$ and the shape of the EA signal over a relatively large voltage range. Section IV contains a summary and conclusions.

## II. EXPERIMENTAL METHOD

The devices studied contain a polyfluorene (PF) based polymer (from the Lumation™ Blue Series, supplied by Sumation Co., Ltd.) with randomly copolymerized triarylamine (TAA) monomer units (7.5 mol %) as the semiconducting layer (PF-TAA), with 67, 98, and 122 nm layer thicknesses. The PF-TAA layer thicknesses were determined from step-height measurements using a Veeco™ Dektak stylus profilometer. The hole transport takes place via the TAA units.[27] The full layer structure and the structure of the fluorene and TAA units are shown in Fig. 1. The anode consists of a 100 nm thick poly(3,4-ethylenedioxythiophene):poly(styrenesulphonic acid) (PEDOT:PSS) layer, spin-coated on precleaned glass substrates covered with 100 nm indium tin oxide (ITO). The cathode consists of a palladium layer, evaporated in a high-vacuum chamber to form 100 nm thick top electrodes. The use of patterned bottom and top electrodes results in glass | ITO | PEDOT:PSS | PF-TAA | Pd structures with areas of $3\times3$ mm$^2$.

Within the EA measurements, a laser beam is focused on the organic diode which is driven by a Keithley 2601 function generator. The applied voltage consists of a dc voltage component, $V_{dc}$, and an ac component with a frequency $f=1.18$ kHz and amplitude $V_{ac}$, so that $V(t)=V_{dc}+V_{ac}\cos 2\pi ft$. The resulting modulation of the reflection is extracted using a Stanford Research Systems SR830 DSP lock-in amplifier, synchronized by the function generator. The use of a Nirvana autobalanced dual-beam photoreceiver, which takes out the dc component of the reflected signal proportional to the incident light intensity, was found to improve the signal-to-noise ratio. The amplitude of the first-order term $R_{ac}\cos 2\pi ft$ in the time-dependent detector response, which is proportional to $-dR/dV$ for sufficiently small values of $V_{ac}$, is usually called "the electroabsorption signal." In a typical measurement, the EA signal is measured as a function of $V_{dc}$, while keeping $V_{ac}$ at a small constant value ~0.8 V. Consistent with the results of Bodrozic *et al.*,[19] no change except for an enhancement of the signal strength was found by increasing $V_{ac}$ up to this value. Also, a variation in the modulation frequency in the range 500–3000 Hz was found to have no effect on the EA signal. This implies that a possible contribution due to charge-induced absorption[15–18,24–26] can be neglected. Furthermore, no hysteresis of the EA signal as a function of the voltage was observed.

The third order susceptibility is proportional to a linear combination of the first and second order derivative of the absorption coefficient with respect to the photon energy.[28] The absorption coefficient of PF-TAA varies strongly in the range from 400 to 450 nm. We studied all three devices using laser diodes with emission wavelengths of 408 and 440 nm. Very similar voltage dependences of the EA signal were obtained, except for the thickest device. In that case, the intensity of the reflected light at 408 nm was rather low due to the relatively high total absorption for that wavelength in the 122 nm organic layer, leading to a relatively poor signal-to-noise ratio. The lower absorptance at 440 nm led to a significantly higher signal-to-noise ratio for measurements at that wavelength. All results reported in this paper have therefore been obtained using the 440 nm laser diode. A systematic variation in the laser fluence, revealed no effect on the measured value of $V_{0,EA}$ and on the voltage dependence of the EA signal.

## III. EXPERIMENTAL RESULTS AND ANALYSIS

Before carrying out the EA experiments, temperature dependent steady-state $J(V)$ curves were measured in order to determine the value of $V_{bi}$ for all three devices studied. The analysis employs a description of the mobility as given by the Gaussian Disorder Model (GDM), using the carrier density and field dependence of the mobility as described in Ref. 7 and with the parameter values describing the mobility as obtained by van Mensfoort *et al.*[8] The inset in Fig. 2 shows the measured and modeled $J(V)$ curves for each thickness, at $T=295$ K. As compared to the earlier study of the same devices in Ref. 8, no change in these curves apart from a slight (~0.2 eV) decrease of $V_{bi}$ was found. The results are included in Table I. From the vacuum work functions of PEDOT:PSS and palladium, which are both close to 5 eV, a built-in voltage close to 0 V would be expected. However, the actual values are much larger, in the range 1.6–1.9 V. As no significant injection barrier at the anode was found, which is expected on the basis of the vacuum work functions of PEDOT:PSS and the very similar ionization potential of the hole-transporting TAA units, the high value of $V_{bi}$ indicates that important metal-organic interactions occur at the cathode interface.[8] The small variation of $V_{bi}$ with $L$ suggests a sensitivity to the (nominally identical) deposition conditions,

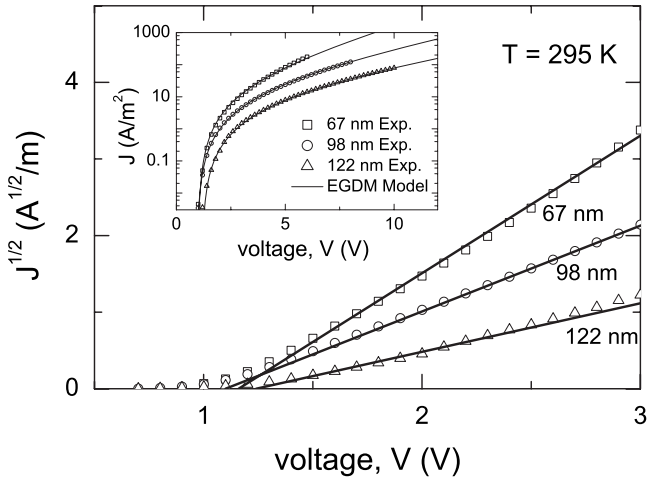


FIG. 2. Square root of the measured current density versus voltage for three PF-TAA layer thicknesses (open symbols) at room temperature, and linear fits through these data taking $J=0$ at $V=V_{0,EA,exp}$ (full lines). The inset shows the corresponding measured data (open symbols) and the modeled current density versus voltage curves (full curves).

and the slightly lower value of $V_{bi}$ as compared to the previous result suggests a small time-dependent change in the dipole layer at the PF-TAA/Pd interface.

Figure 3 shows the measured EA signal (squares) for the three PF-TAA layer thicknesses. Two observations can be made immediately. First, the measured zero-crossing values $V_{0,EA}$ (included in Table I) are significantly smaller then the built-in voltages as determined above (red squares). A qualitatively similar result was recently found by Gather *et al.*,[25] who studied devices containing a green-emitting phosphorescent polymer/dye blend and measured an EA zero crossing at ~2.5 V whereas a value of ~3.0 V was expected on the basis of the work function difference of the electrodes. In that work, no further analysis was given. Second, the shape of the voltage dependence of the signal changes with the thickness: for the 67 nm device the curve is slightly concave

TABLE I. Layer thickness dependence of the built-in voltage ($V_{bi}$), the zero-crossing voltage as determined from EA experiments ($V_{0,EA,exp}$) and as calculated using the model discussed in Sec. III ($V_{0,EA,mod}$), and the peak voltage as obtained from low-frequency differential capacitance measurements ($V_{p,C}$). $V_{0,EA,mod}$ was calculated by subtracting from $V_{bi}$ the value of $V_{bi}$-$V_{0,EA,mod}$ as obtained from modeling.

| $L$ (nm) | $V_{bi}$ (V) | $V_{0,EA,exp}$ (V) | $V_{0,EA,mod}$ $V_{bi}$-$V_{0,EA,mod}$ (V) | $V_{p,C}$ (V) |
|---|---|---|---|---|
| 67 | $1.66\pm0.05$ | $1.16\pm0.07$ | $1.18\pm0.10$ | $1.10\pm0.04$ |
| | | | $0.48\pm0.05$ | |
| 98 | $1.63\pm0.05$ | $1.10\pm0.10$ | $1.08\pm0.10$ | $1.00\pm0.03$ |
| | | | $0.55\pm0.05$ | |
| 122 | $1.87\pm0.05$ | $1.24\pm0.15$ | $1.29\pm0.10$ | $1.2\pm0.1$ |
| | | | $0.58\pm0.05$ | |

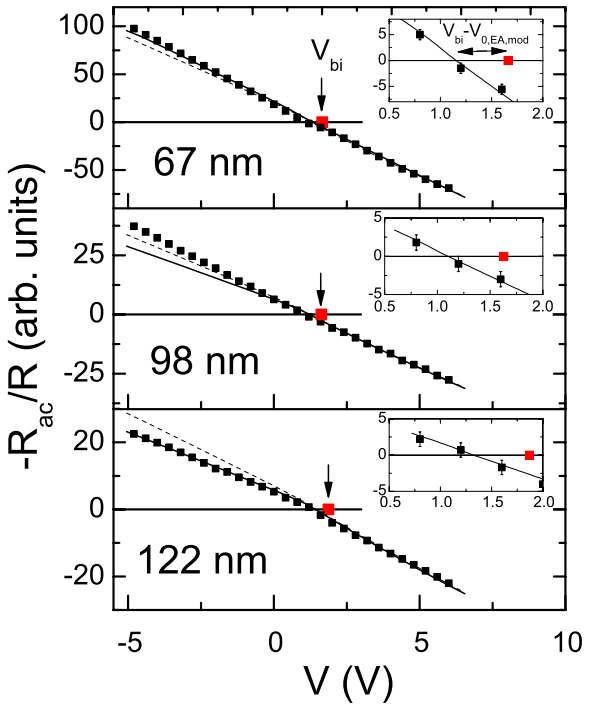


FIG. 3. (Color online) Electroabsorption signal as a function of the bias voltage for three devices with different PF-TAA layer thicknesses. Black small squares: experimental data. The arrows and the larger red squares indicate the values of the built-in voltage as determined from an analysis of steady state current-voltage curves. Full and dashed curves: model results including and excluding the position dependence of the absorptance rate, respectively (see text). The insets provide a closer view around $V_{0,EA}$.

whereas it is slightly convex for the 122 nm device. A nonlinear shape of the EA signal was also found in other studies,[20,25] and was argued to be due to screening of the internal field resulting from space charge injected in the device or to a voltage dependent contribution due to charge-induced absorption. However, no quantitative analysis was given. The observed difference between $V_{0,EA}$ and $V_{bi}$ and the voltage dependence of the EA signal are the two issues we will clarify by modeling the measured EA signals. We note that the shape of the signal versus voltage does not yield any indication for a possible effect of electron trapping at the anode interface, in contrast to the results obtained by Brewer *et al.*[15,16,18] for poly(9,8-dioctyl)fluorene (PFO) based devices, i.e., for a polymer without TAA hole transporting units.

The observation of an EA signal which varies linearly with the voltage is commonly viewed as a justification of the assumption that the device is space-charge free. However, the fact that the detailed shape of the curves depends on the layer thickness indicates that this point of view is in general not correct, and that even in the case of near-linearity this can be the result of an interplay between various balancing effects. In the devices studied, there is already at zero applied voltage a considerable space charge present in the PF-TAA layer near the anode interface, which forms a well-injecting contact for holes due to the low or even negligible injection barrier at that interface.[8] In order to investigate the effect of

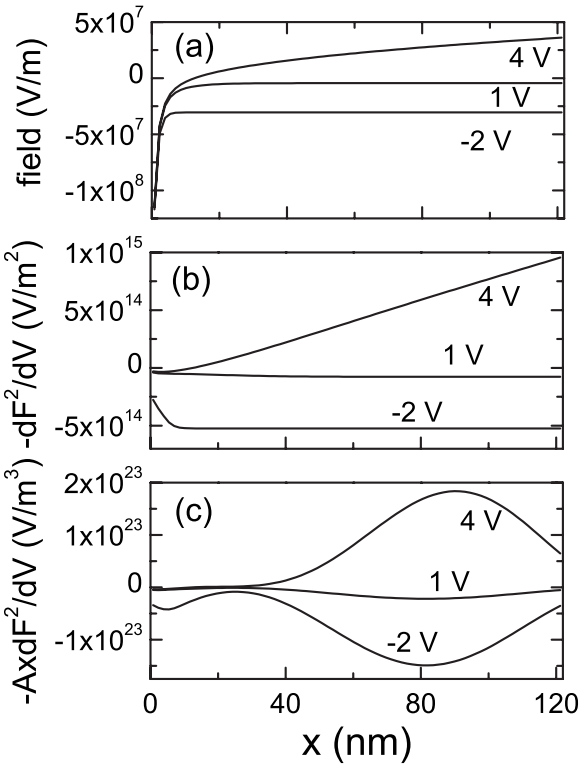


FIG. 4. Calculated variation in the electric field $F$ (a), the function $-dF^2/dV$ (b), and the function $-A \times dF^2/dV$ (c) throughout a 122 nm PF-TAA layer in the devices studied for several applied voltages.

this space charge on the EA signal, as a first step the position-dependent electric field $F(x)$ is calculated as a function of the voltage, using the drift-diffusion model given in Ref. 29. Figure 4(a) shows results for a 122 nm thick PF-TAA layer, for three values of the voltage. The figure clearly reveals a strong position dependence of the field in at least a part of the device.

In the case of a nonuniform electric field, the EA signal is affected by the position dependence of the absorptance rate $A(x)$, defined as the fraction of the incident radiant energy absorbed per nanometer. Under the conditions employed, the relative change in the light absorption in the device upon modulating the bias voltage is very small. The voltage dependence of the EA signal may then be expressed as

$$\frac{R_{ac}}{R}(h\nu, V) \propto -\mathrm{Im}\,\chi^{(3)}(h\nu)\int_0^L A(x)\left.\frac{dF(x,V')^2}{dV'}\right|_V dx. \quad (2)$$

Figure 4(b) shows for the 122 nm device the calculated position dependence of the function $dF^2/dV$. Figure 1 shows the absorptance rate for a 440 nm incident wavelength, as used in the EA experiments, for the case of a constant absorption coefficient corresponding to $F(x)=0$. The calculation has been carried out using the thin-film optical software package MACLEOD, with the complex refractive indices of the layers as determined by ellipsometry. The light absorption in the PF-TAA layer is quite nonuniform. As a result, changes in the absorption coefficient at a position of about 40 nm from the Pd electrode, for example, contribute more strongly to the EA signal than changes close to the LEP-Pd interface. Figure 4(c) gives the position dependence of the absorptance-weighed contributions to the EA signal.

Application of Eq. (2) leads to the full model curves shown in Fig. 3. The model results obtained by only taking the position dependence of the electric field into account [i.e., assuming $A(x)=1$], are shown by dashed curves. In all cases, the proportionality factor is taken such that an optimal fit is obtained for positive voltages. The insets show the same results, focusing at the region around $V_{0,EA}$. The values of $V_{0,EA}$ as obtained from the model are included in Table I. Excellent agreement is obtained with the experimental zero-crossing voltages. Furthermore, it is seen from the figure that both model curves yield essentially the same value of $V_{0,EA}$, but that the full shape of the EA curves is affected by the position dependence of the absorptance. Including the absorptance in the model improves the description of the voltage dependences of the EA signal for the 67 and 122 nm devices. From the experiment, the EA curves are slightly convex and concave, respectively. On the other hand, including the absorptance leads for the 98 nm device to slightly worse agreement with experiment. We find that for this layer thickness a shift in the absorption profile of only 12 nm toward the middle of the devices would give rise to a (more concave) shape of the EA curve which agrees excellently with the experimental curve. The analysis of the full shape of the curves (but in this case not the determination of $V_{0,EA}$) is thus very sensitive to the exact form of the absorptance profile. The occurrence of a small shift in the absorption profile may in practice be induced by a slightly lower reflection at the polymer-Pd interface due to, for example, interface roughness.

The zero-crossing voltage as determined from EA can thus be considerably smaller than the built-in voltage. The effect is a result of the presence of space charge in the organic semiconductor. Although the space-charge density is largest near the anode, its presence throughout the entire device is non-negligible. Therefore, the difference between $V_{bi}$ and $V_{0,EA}$ is layer thickness dependent. The experimentally observed difference increases from 0.50 V for the 67 nm device to 0.63 V for the 122 nm device, consistent with the model predictions. Although it is thus incorrect to associate $V_{0,EA}$ to $V_{bi}$, we find that it is still possible to view $V_{0,EA}$ as an effective onset value of the space-charge-limited current. This may be seen from Fig. 2, which shows that in the voltage range in between $V_{0,EA}$ and $V_{bi}$ good linear fits can be made to the square-root of the current density, taking the voltage at which the curves extrapolate to zero equal to $V_{0,EA}$.

It has previously been established that an alternative measure for the effective onset voltage is given by the voltage $V_{p,C}$ at which at low frequencies a distinct peak in the differential capacitance is observed.[5] The values of $V_{p,C}$, as obtained from differential capacitance measurements at frequencies from 100 up to 5000 Hz, are included in Table I. They are indeed close to the values of $V_{0,EA}$. The finding that $V_{p,C}$ is slightly larger for the 122 nm device than for the two other devices is consistent with the finding of a slightly larger value of $V_{bi}$ for that device.

It would be of interest to extend in future studies the EA experiments to lower temperatures. The effect of charge-carrier diffusion on $V_{0,EA}$ is expected to decrease with decreasing temperature, as it is due to space charge in the device. A similar effect has already been observed by Kemerink *et al.*[30] for the temperature dependence of the onset voltage in poly-phenylene-vinylene (PPV) based devices. To our point of view, the built-in voltage is then given by the value of the onset voltage, extrapolated to zero temperature.

## IV. CONCLUSIONS

We have studied hole-only devices based on a PF-TAA copolymer with a very small injection barrier at the anode interface, and have shown that the voltage at which the EA signal vanishes is significantly smaller than the built-in voltage, determined from the analysis of the steady-state current density curves. The difference depends on the device thickness, and can be understood as a result of charge-carrier diffusion, which leads to a strong variation in the electric field throughout the LEP layer. It has been shown that the zero-crossing voltage essentially coincides with the effective onset of the space-charge-limited current density, and with a distinct peak in the differential capacitance. A similar effect is known from studies of photovoltaic cells, where in the absence of extraction barriers the open-circuit voltage $V_{oc}$ can be 0.5 eV smaller than $V_{bi}$.[31] The shape of the voltage dependence of the measured EA signal, which is concave and convex for the device with a 67 and 122 nm LEP layer, respectively, can be understood well by properly taking the variation in the absorptance throughout the organic layer into account. The analysis of the detailed shape of the EA curves is found to be quite sensitive to the detailed shape of the absorptance profiles, which therefore in general should be taken into account when analyzing the results of EA measurements.

## ACKNOWLEDGMENTS

The authors wish to thank G. 't Hooft for useful advice on the experimental setup, and Sumation Co., Ltd for the supply of Lumation™ Blue Series polymers. This work forms part of the research program of the DPI (Project No. 680). The research has also received funding from NanoNed, a national nanotechnology program coordinated by the Dutch Ministry of Economic Affairs (contribution S.L.M.v.M.), and from the European Community's Seventh Framework Program under Grant No. 213708 (AEVIOM, contribution R.C.).

*rein.de.vries@philips.com

[1] C. W. Tang and S. A. VanSlyke, Appl. Phys. Lett. **51**, 913 (1987).
[2] Y. Sun, N. C. Giebink, H. Kanno, B. Ma, M. E. Thompson, and S. R. Forrest, Nature (London) **440**, 908 (2006).
[3] S.-J. Su, E. Gonmori, H. Sasabe, and J. Kido, Adv. Mater. **20**, 4189 (2008).
[4] S. Reineke, F. Lindner, G. Schwartz, N. Seidler, K. Walzer, B. Lüssem, and K. Leo, Nature (London) **459**, 234 (2009).
[5] S. L. M. van Mensfoort and R. Coehoorn, Phys. Rev. Lett. **100**, 086802 (2008).
[6] G. G. Malliaras, J. R. Salem, P. J. Brock, and J. C. Scott, J. Appl. Phys. **84**, 1583 (1998).
[7] W. F. Pasveer, J. Cottaar, C. Tanase, R. Coehoorn, P. A. Bobbert, P. W. M. Blom, D. M. de Leeuw, and M. A. J. Michels, Phys. Rev. Lett. **94**, 206601 (2005).
[8] S. L. M. van Mensfoort, S. I. E. Vulto, R. A. J. Janssen, and R. Coehoorn, Phys. Rev. B **78**, 085208 (2008).
[9] I. H. Campbell, T. W. Hagler, D. L. Smith, and J. P. Ferraris, Phys. Rev. Lett. **76**, 1900 (1996).
[10] C. M. Heller, I. H. Campbell, D. L. Smith, N. N. Barashkov, and J. P. Ferraris, J. Appl. Phys. **81**, 3227 (1997).
[11] T. M. Brown, J. S. Kim, R. H. Friend, F. Cacialli, R. Daik, and W. J. Feast, Appl. Phys. Lett. **75**, 1679 (1999).
[12] T. M. Brown, R. H. Friend, I. S. Millard, D. L. Lacey, T. Butler, J. H. Burroughes, and F. Cacialli, J. Appl. Phys. **93**, 6159 (2003).
[13] S. J. Martin, G. L. B. Verschoor, M. A. Webster, and A. B. Walker, Org. Electron. **3**, 129 (2002).
[14] P. A. Lane, P. J. Brewer, J. Huang, D. D. C. Bradley, and J. C. deMello, Phys. Rev. B **74**, 125320 (2006).
[15] P. J. Brewer, P. A. Lane, J. deMello, D. D. C. Bradley, and J. C. deMello, Adv. Funct. Mater. **14**, 562 (2004).
[16] P. J. Brewer, P. A. Lane, J. Huang, A. J. deMello, D. D. C. Bradley, and J. C. deMello, Phys. Rev. B **71**, 205209 (2005).
[17] P. J. Brewer, A. J. deMello, J. C. deMello, P. A. Lane, D. D. C. Bradley, R. Fletcher, and J. O'Brien, J. Appl. Phys. **99**, 114502 (2006).
[18] P. J. Brewer, J. Huang, P. A. Lane, A. J. deMello, D. D. C. Bradley, and J. C. deMello, Phys. Rev. B **74**, 115202 (2006).
[19] V. Bodrozic, M. Roberts, N. Philips, J. H. Burroughes, S. Mian, and F. Cacialli, J. Appl. Phys. **101**, 084507 (2007).
[20] C. V. Hoven, J. Peet, A. Mikhailovsky, and T. Nguyen, Appl. Phys. Lett. **94**, 033301 (2009).
[21] D. E. Aspnes and J. E. Rowe, Phys. Rev. B **5**, 4022 (1972).
[22] I. H. Campbell, M. D. Joswick, and I. D. Parker, Appl. Phys. Lett. **67**, 3171 (1995).
[23] F. Rohlfing, T. Yamada, and T. Tsutsui, J. Appl. Phys. **86**, 4978 (1999).
[24] K. Book, H. Bässler, A. Elschner, and S. Kirchmeyer, Org. Electron. **4**, 227 (2003).
[25] M. C. Gather, R. Jin, J. de Mello, D. D. C. Bradley, and K. Meerholz, Appl. Phys. B: Lasers Opt. **95**, 113 (2009).
[26] I. H. Campbell, D. L. Smith, C. J. Neef, and J. P. Ferraris, Appl. Phys. Lett. **78**, 270 (2001).
[27] R. J. de Vries, S. L. M. van Mensfoort, V. Shabro, S. I. E. Vulto, R. A. J. Janssen, and R. Coehoorn, Appl. Phys. Lett. **94**, 163307 (2009).
[28] S. J. Martin, D. D. C. Bradley, P. A. Lane, H. Mellor, and P. L. Burn, Phys. Rev. B **59**, 15133 (1999).
[29] R. Coehoorn and S. L. M. van Mensfoort, Phys. Rev. B **80**, 085302 (2009).
[30] M. Kemerink, J. M. Kramer, H. H. P. Gommans, and R. A. J. Janssen, Appl. Phys. Lett. **88**, 192108 (2006).
[31] V. D. Mihailetchi, P. W. M. Blom, J. C. Hummelen, and M. T. Rispens, J. Appl. Phys. **94**, 6849 (2003).